

Synthesis, Characterization, and Computational Studies of Cycloparaphenylene Dimers

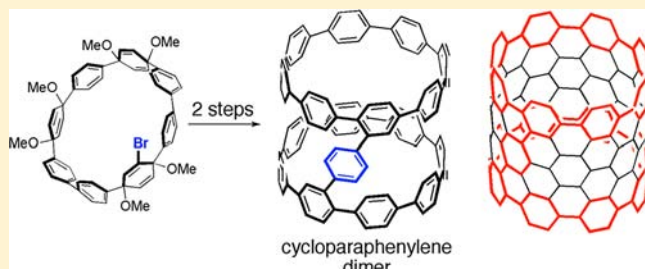
Jianlong Xia,[†] Matthew R. Golder,[†] Michael E. Foster,[‡] Bryan M. Wong,[‡] and Ramesh Jasti^{*,†}

[†]Department of Chemistry, Boston University, 24 Cummington St., Boston, Massachusetts 02215, United States (USA)

[‡]Materials Chemistry Department, Sandia National Laboratories, Livermore, California 94551, United States (USA)

Supporting Information

ABSTRACT: Two novel arene-bridged cycloparaphenylene dimers (**1** and **2**) were prepared using a functionalized precursor, bromo-substituted macrocycle **7**. The preferred conformations of these dimeric structures were evaluated computationally in the solid state, as well as in the gas and solution phases. In the solid state, the trans configuration of **1** is preferred by 34 kcal/mol due to the denser crystal packing structure that is achieved. In contrast, in the gas phase and in solution, the cis conformation is favored by 7 kcal/mol (dimer **1**) and 10 kcal/mol (dimer **2**), with a cis to trans activation barrier of 20 kcal/mol. The stabilization seen in the cis conformations is attributed to the increased van der Waals interactions between the two cycloparaphenylene rings. These calculations indicate that the cis conformation is accessible in solution, which is promising for future efforts toward the synthesis of short carbon nanotubes (CNTs) via cycloparaphenylene monomers. In addition, the optoelectronic properties of these dimeric cycloparaphenylenes were characterized both experimentally and computationally for the first time.



INTRODUCTION

Since their discovery in 1991,¹ carbon nanotubes (CNTs) have captured the interest of physicists, engineers, and chemists due to their unique architecture, desirable optoelectronic properties, as well as their high tensile strength.² Over the last two decades, chemical vapor deposition³ and laser ablation methods⁴ have been developed further, allowing for the scalable production of carbon nanotubes. These synthetic methods, however, provide very little control over CNT diameter or chirality — the two structural features that determine the band gap of CNTs.^{2,5} To take advantage of the unique properties of CNTs for applications in nanotechnology, new synthetic approaches to circumvent these shortcomings must be pursued.^{6–9}

The [*n*]cycloparaphenylenes ([*n*]CPPs) represent the shortest possible fragment of an [*n,n*]armchair carbon nanotube (CNT). Because of this structural relationship, the CPPs have recently attracted significant attention due to their potential as monomeric precursors or seeds for the bottom-up synthesis of uniform [*n,n*]armchair CNTs.^{5–8,10–19} Additionally, CPPs exhibit size-dependent, tunable optoelectronic properties,^{16,20–26} which position them as novel carbon quantum dots for optoelectronic applications.²³ Furthermore, the cycloparaphenylenes possess unique nanosized cavities which can be exploited for supramolecular assemblies^{25,27} or as components of novel graphitic materials and porous organic frameworks. With these promising features in mind, the CPPs have become highly touted non-natural synthetic targets.

Only recently have the cycloparaphenylenes succumbed to synthesis. As early as 1934, well before the discovery of CNTs,

the [*n*]CPPs were first conceptualized and the initial attempts were made at their preparation.²⁸ These highly strained aromatic macrocycles were later revisited by Vögtle and co-workers in 1993, but they too were unsuccessful in synthesizing the desired [*n*]CPPs.²⁹ It was not until 2008 that the CPPs were finally prepared by Jasti and Bertozzi utilizing novel reductive aromatization methodology.²² Since then, our group,^{22–25,30} as well as the groups of Itami^{16,31–35} and Yamago,^{21,36,37} have made the synthetic availability of [*n*]CPPs (*n* = 6–16, 18) possible. Most recently, our group has developed the gram-scale synthesis of two different sized CPPs, heightening the interest in using these fascinating structures in materials science applications and as possible precursors to uniform CNTs.³⁸

Despite recent contributions by Itami,^{16,31–35} Yamago,^{21,36,37} and our group,^{22–25,30} a synthetic procedure toward the functionalization of cycloparaphenylenes has not been reported to date. In particular, synthetic methods that can connect CPP units may allow access to wider polyaromatic hydrocarbon belts and ultimately CNTs. Herein, we describe the first synthesis of arene-bridged cycloparaphenylene dimers (Figure 1) as well as their optoelectronic characterization (Figure 2). We also report computational studies indicating that in the gas phase and in solution these arene-bridged cycloparaphenylene dimers prefer cis conformations in which the two cycloparaphenylene units are stacked on top of each other in a nanotube-like geometry.

Received: July 26, 2012

Published: November 6, 2012

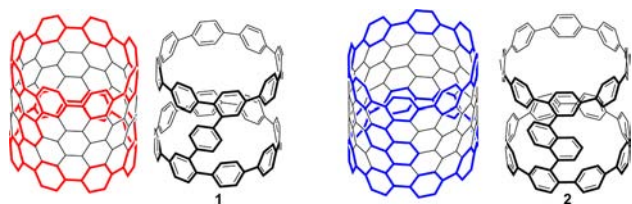


Figure 1. Cycloparaphenylene dimers are short segments of armchair carbon nanotubes.

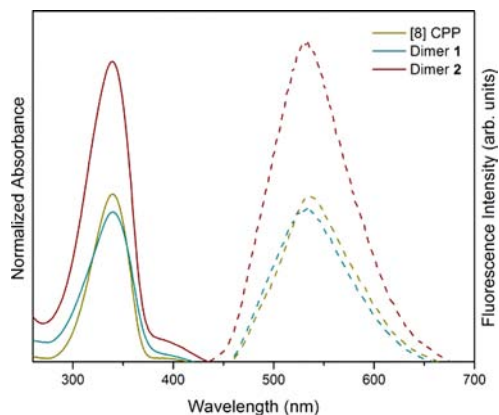


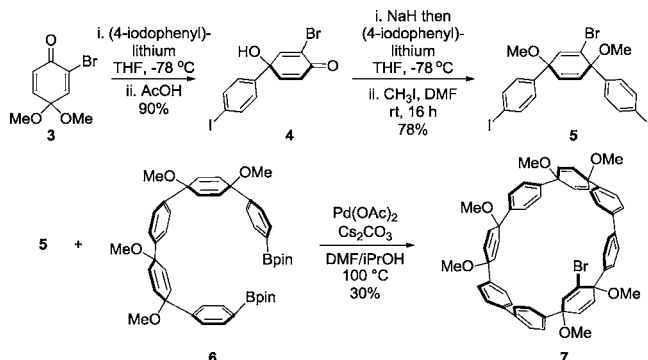
Figure 2. Normalized UV-vis absorption (solid line) and fluorescence spectra (dashed line) of 1, 2 and [8]CPP in dichloromethane.

This result along with synthetic access to linked CPP structures opens up the possibility of using these dimeric structures to synthesize short CNT fragments via cycloparaphenylene monomers. More broadly, the synthetic methodology developed in this work will be amenable to preparing a wide variety of monofunctionalized CPPs for use in materials science applications.

RESULTS AND DISCUSSION

Synthesis and Characterization. To couple two cycloparaphenylene molecules, installation of a functional handle for dimerization was required. We hypothesized that a late-stage functionalization reaction of CPP would likely lead to mixtures so we turned our attention to preparing a monofunctionalized macrocyclic precursor. We envisioned bromo-substituted macrocycle 7 as a key intermediate — a structure that could be further derivatized through transition metal catalyzed cross-coupling reactions (Scheme 1). Recently, we reported a sequential oxidative dearomatization/addition procedure using

Scheme 1. Synthesis of Bromo-Substituted Macrocyclic 7

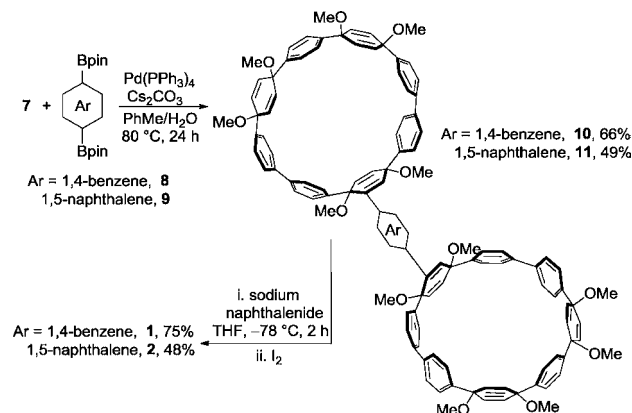


cyclohexadiene units as masked benzene rings to prepare compound 6 on multigram scale. This building block was successfully used in the synthesis of [6]cycloparaphenylene,²⁴ the smallest CPP to date, as well as the first gram-scale synthesis of [8]CPP and [10]CPP.²⁵ We expected that bromo-substituted macrocycle 7 could be prepared efficiently by taking advantage of readily available building block 6.

Diiodide 5 (Scheme 1), which bears a vinyl bromide functionality within the cyclohexadiene unit, is easily prepared in two steps. The synthesis started from 2-bromo-4,4-dimethoxycyclohexa-2,5-dienone 3,³⁹ which underwent an addition of (4-iodophenyl)lithium, and subsequent deprotection with 10% AcOH to generate bromodienone 4 in 90% yield. Deprotonation of alcohol 4 with sodium hydride followed by addition of (4-iodophenyl)lithium, and subsequent methylation in a one-pot sequence²⁵ produced brominated monomer 5 in 78% yield and in high diastereoselectivity. Diiodide 5 and diboronate 6^{24,25} underwent Suzuki coupling/macrocyclization in the presence of Pd(OAc)₂ (0.1 equiv), Cs₂CO₃ (4 equiv) in DMF/iPrOH (10:1) at 100 °C for 24 h to deliver macrocycle 7 in 30% isolated yield. Notably, the less reactive vinyl bromide remained intact under these reaction conditions.

With bromo-substituted macrocycle 7 in hand, we next investigated the reactivity of the vinyl bromide for metal-catalyzed cross-coupling reactions to prepare macrocyclic precursors to arene-bridged dimers 1 and 2 (Scheme 2).

Scheme 2. Dimerization and Reductive Aromatization to Synthesize 1 and 2



After careful exploration, we found that macrocycle 7 and commercially available 1,4-benzenediboronic acid bis(pinacol) ester 8 underwent an efficient Pd-catalyzed cross-coupling reaction in the presence of Pd(PPh₃)₄/Cs₂CO₃ in toluene/H₂O at 80 °C for 24 h to deliver the dimeric macrocycle 10 in 66% isolated yield. Under the same conditions, the 1,5-naphthalene bridged dimeric macrocycle 11 was also assembled by coupling of 7 with 1,5-naphthalenediboronic acid bis(pinacol) ester⁴⁰ 9 in 49% yield.

Subjecting 10 and 11 to sodium naphthalenide²⁵ at −78 °C for 2 h and then quenching with I₂ led to the arene-bridged CPPs 1 and 2 in 75% and 48% isolated yield, respectively. Both compounds exhibit clusters of overlapping peaks around 127.4 and 137.8 ppm in the ¹³C NMR spectra — consistent with the chemical shifts observed for [8]CPP.²¹ The ¹H NMR spectra of both compounds exhibit multiple overlapping peaks ranging from 7–8 ppm as expected. The MALDI-TOF mass spectra of

1 and **2** show single peaks at 1291.5924 and 1341.1713, respectively.

Optoelectronic Characterization. With the CPPs possessing unique optoelectronic properties, we were curious about the behavior of these novel dimeric structures. Both **1** and **2** exhibit an absorption maximum at 340 nm, similar to that of [8]CPP and other CPPs (Figure 2). The extinction coefficient (ϵ) of dimer **1** is $0.87 \times 10^{-5} \text{ M}^{-1} \text{ cm}^{-1}$, which is slightly smaller than that of [8]CPP ($\epsilon = 1.0 \times 10^{-5} \text{ M}^{-1} \text{ cm}^{-1}$),²¹ while dimer **2** exhibits an increased ϵ value of $1.7 \times 10^{-5} \text{ M}^{-1} \text{ cm}^{-1}$ (Figures S1 and S2 of the Supporting Information). The corresponding emission spectra have the same maximum as [8]CPP at about 540 nm (Figure 2), with improved fluorescence quantum yields of 0.18 and 0.15 (Figures S3 and S4 of the Supporting Information) respectively in contrast to that of [8]CPP (0.10).³⁰ The enhanced quantum yields may indicate a more rigid structure. Cyclic voltammetry analysis showed that the half-wave oxidation potentials of **1** and **2** are 0.64 and 0.68 V (vs Fc/Fc⁺), which are larger than that of [8]CPP (0.59 V).²¹

COMPUTATIONAL STUDIES

Conformational Analyses. With the first cycloparaphenylene dimers in hand, we were interested in the conformational dynamics of these molecules in solution. One can envision two extreme orientations — a trans conformer in which the two CPP rings are positioned as far apart as possible from each other (Figure 4, leftmost structure) or a cis conformer in which

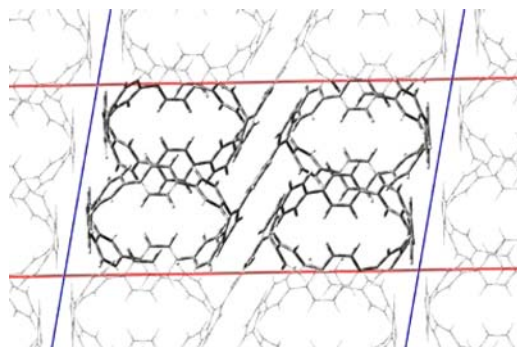


Figure 3. Optimized (PBE-D functional) solid state packing of trans **1**.

the CPP rings are oriented on top of each other in a nanotube-like arrangement (Figure 4, rightmost structure). If the cis conformer is accessible in solution, further oxidative carbon–carbon bond forming reactions (e.g., Scholl reaction) may be feasible to lock the molecule into a nanotube-like geometry. In addition to this enticing possibility, the dimeric CPPs can also be envisioned as supramolecular host molecules which can readily switch orientation.^{41–47} The energetics and pathways for this conformational isomerization are relevant for both types of future studies. In an effort to unravel the conformational dynamics of these molecules, we first considered NMR analysis. Unfortunately, the high levels of symmetry in these molecules impede this type of study. Therefore, we decided to investigate these issues *in silico* (vide infra).

As an initial starting point for our investigations, we decided to examine the solid state structure of these dimeric CPPs. Accordingly, several attempts were made to acquire the crystal structures of dimers **1** and **2**. Unfortunately, due to the insolubility of these compounds, only very small, weakly

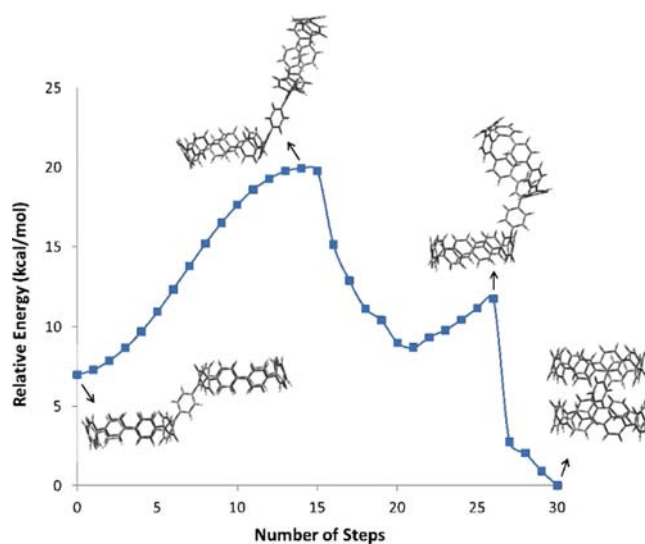


Figure 4. Potential energy curve (B3LYP-D/6-31G(d,p)) of the trans to cis transition for **1**.

diffracting crystals could be obtained. The samples suffered rapid decomposition during handling due to solvent loss, and further decomposition during X-ray data collection due to radiation damage. The resulting data sets were highly incomplete and although a preliminary solution for dimer **1** clearly showed two linked macrocycles in the trans geometry, the structure could not be refined.⁴⁸ Because of the uncertainty in the crystallographic data, we sought to verify this result computationally by performing periodic boundary condition calculations using the PBE-D functional with projector augmented wave pseudopotential on the experimental crystal structure (trans) (Figure 3) and a representative cis crystal structure (Figure S11 of the Supporting Information). Upon optimization of the unit cell and atomic positions, the trans crystal structure is predicted to be lower in energy by 34 kcal/mol per molecule. In addition, the unit cell volume of the optimized trans structure is smaller by 16% resulting in a denser crystal packing. This computational result is consistent with the preliminary X-ray data that was acquired.

Next, we examined the dynamics of the CPP dimer systems in both the gas phase and in solution. An analysis of the conformational barrier from trans to cis in the gas phase was conducted for **1** using DFT-based *ab initio* calculations.^{49,50} It is important to note that to properly model these nanohoop systems, a computational method capable of modeling van der Waals interactions must be used, such as the B3LYP-D functional. The B3LYP functional alone is incapable of modeling van der Waals interactions and is therefore quantitatively incapable of modeling these types of systems. We also investigated these systems using the M06–2X functional, which, like B3LYP-D, is designed for modeling van der Waals interactions. For both types of calculations, the same quantitative results were achieved.

The potential energy curve (PEC) (Figure 4) corresponding to the trans to cis conformational change in compound **1** was calculated by starting with the optimized trans geometry and creating a series of structures mapping the conformational change (provided movie in the Supporting Information). These structures were optimized, minimizing the total energy, while constraining two dihedral angles (Figure S7 of the Supporting Information). At the B3LYP-D/6-31G(d,p) level of theory, the

energy barrier from trans to cis (i.e., left to right) is 13 kcal/mol. The energy barrier from cis to trans (i.e., right to left) is 20 kcal/mol, in which the lowest energy pathway is that in which one CPP ring flips on top of the other as opposed to a rotating motion around the aryl linker axis (see provided movie in the Supporting Information). In contrast to the solid state structure, the cis conformation is found to be 7 kcal/mol more stable in energy in the gas phase because of the increased van der Waals interactions between the two rings. The cis conformation of dimer **2** is predicted to be 10 kcal/mol lower in energy than the trans conformation (Figure S8 of the Supporting Information). Furthermore, SCRF calculations using a polarizable continuum model (PCM) and the B3LYP-D functional showed no changes in the preferred conformation or relative stability of **1** and **2** via the inclusion of dichloromethane solvent effects. These results together are very promising for future efforts toward the synthesis of short carbon nanotubes via cycloparaphenylene monomers.

Inspired by arene-bridged cycloparaphenylene dimers **1** and **2**, we were also interested in the conformational dynamics of a direct CPP dimer (i.e., no arene-linker) (Figure 5). This

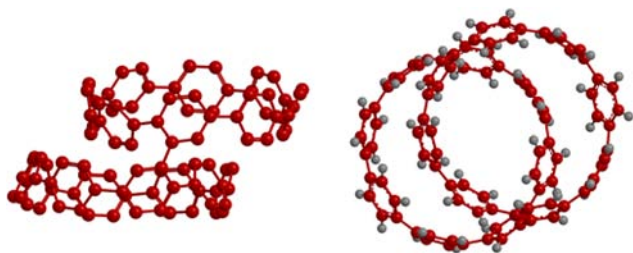


Figure 5. Side-view (left) and top-view (right) of lowest-energy conformation of directly linked [8]CPP dimer.

molecule is especially fascinating because, if it can be prepared, successful cyclodehydrogenation would deliver an ultrashort CNT in one step. To probe this type of structure further, we again analyzed the potential energy surface of the corresponding cis to trans conformational change by DFT calculations (Figure S10 of the Supporting Information). Surprisingly, the trans conformation is predicted to be a relatively unstable local minimum in comparison to the cis conformation, which is predicted to be 30 kcal/mol lower in energy. We therefore propose directly linked CPP dimers as exciting new synthetic targets that our laboratory is actively pursuing.

TD-DFT Calculations. To gain a more in depth understanding of the optical data for the CPP dimers, we carried out TD-DFT calculations at the B3LYP-D/6-31G(d,p) level of theory for both the cis and trans conformations of **1** and **2**. The calculations revealed that although the HOMO→LUMO transition is forbidden for [8]CPP ($f = 0$), the HOMO→LUMO transition of dimers **1** and **2** have nonzero oscillator strengths (Table 1).⁵¹ Consistent with this result, we observe weak shoulder peaks centered around 400 nm for both dimers **1** and **2** that is not present in the absorption spectrum of [8]CPP (vide supra, Figure 2). Furthermore, TD-DFT results indicate that the maximum absorption of the cis conformation of **1** can be assigned to a combination of HOMO-3→LUMO, HOMO→LUMO+2, and HOMO→LUMO+3 transitions, whereas the maximum absorption for cis **2** can be assigned to HOMO-4→LUMO, HOMO-3→LUMO, and HOMO→LUMO+3. The maximum absorption of the trans conformation at approximately 375 nm can be attributed to a blending of

Table 1. Significant Optical Contributions Obtained via TD-DFT Calculations^a

| | Major Contributions ^b | Osc. Strength | Wavelength (nm) |
|--------------|----------------------------------|---------------|-----------------|
| | H→L | 0 | 473 |
| | H-1→L | 1.4872 | 356 |
| [8] CPP | H→L+1 | 1.4872 | 356 |
| | H-2→L | 1.3057 | 345 |
| | H→L+2 | 1.3057 | 345 |
| <i>cis</i> | H→L | 0.0084 | 481 |
| | H→L+2 | 0.2574 | 365 |
| Dimer 1 | H→L+3 | 0.2574 | 365 |
| | H→L | 0.0085 | 467 |
| | H→L+2 | 1.0170 | 379 |
| <i>trans</i> | H-2→L | 0.7106 | 373 |
| <i>cis</i> | H→L | 0.0146 | 479 |
| | H-4→L | 0.1236 | 368 |
| | H-3→L | 0.1236 | 368 |
| Dimer 2 | H→L+3 | 0.1236 | 368 |
| | H→L | 0.0199 | 465 |
| | H→L+2 | 0.4018 | 379 |
| <i>trans</i> | H-2→L | 0.6321 | 373 |

^aCalculations were performed at the B3LYP-D/6-31G(d,p) level of theory. ^bH = HOMO, L = LUMO.

HOMO-2→LUMO and HOMO→LUMO+2 transitions for both **1** and **2**. TD-DFT calculations predict very similar optical absorption spectra for both the cis and trans conformers of dimers **1** and **2**. Hence, the preferred conformations of **1** and **2** in solution could not be addressed by analysis of the UV-vis data and TD-DFT calculations.

In addition to the TD-DFT calculations, we also analyzed the frontier molecular orbitals of dimer **1** (Figure 6). In contrast to the predicted absorption spectra, the frontier molecular orbitals of the cis and trans configurations of **1** are localized quite differently. Most notably, in the cis configuration (C_1 symmetry), the HOMO and LUMO lie almost exclusively on one cycloparaphenylene ring on either side of the arene bridge. However, the HOMO and LUMO are more evenly distributed across the arene bridge in the higher symmetry (C_i) trans configuration. An FMO analysis on dimer **2** led to similar results (Figure S10 of the Supporting Information). The higher level of symmetry in the trans conformers is also responsible for the larger oscillator strengths compared to the cis conformers (Table 1).

CONCLUSIONS

In summary, the syntheses of arene-bridged CPP dimers **1** and **2** were accomplished using macrocycle precursor **7**. More broadly, this general synthetic route will be useful for the preparation of a variety of monofunctionalized CPPs via cross-

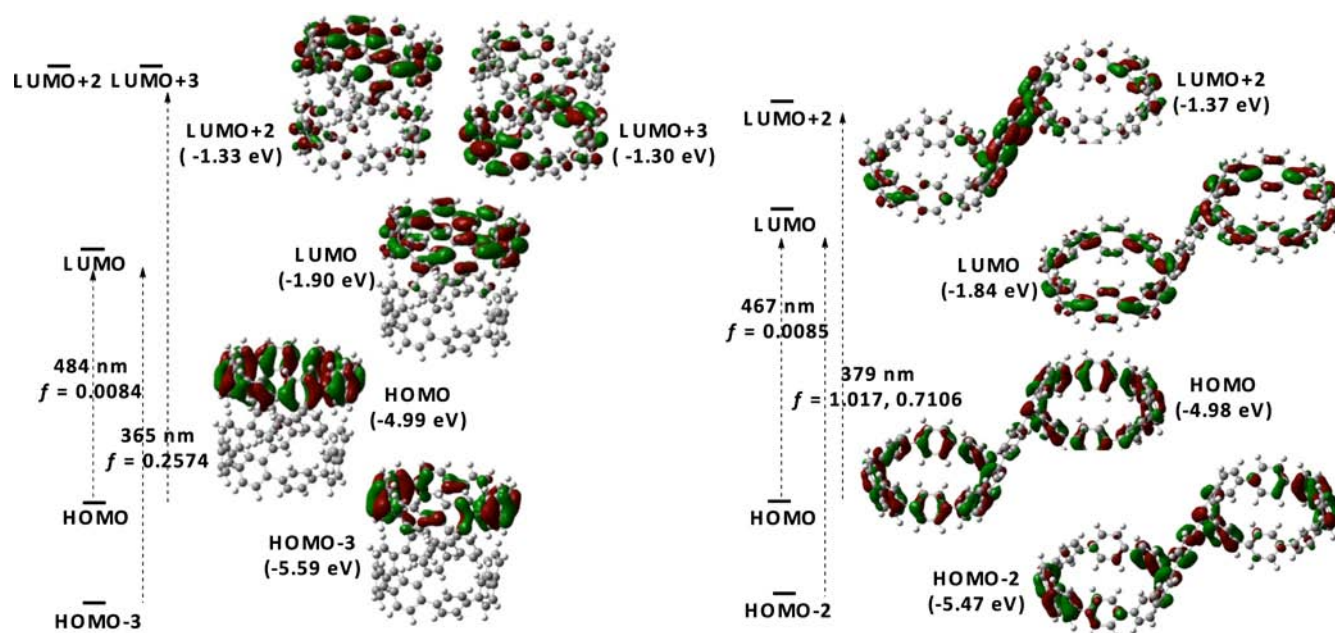


Figure 6. Major electronic transitions (TD-DFT) and representative FMOs for **1** cis (left) and trans (right), calculated at the B3LYP/6-31G(d,p) level of theory.

coupling reactions. From computational analyses, we find that **1** and **2** can adopt favored cis conformations in the gas phase and in solution, although the trans is the preferred conformer in the solid state. As a result, further carbon–carbon bond forming reactions (e.g., cyclodehydrogenations) that lock the cis conformation and generate a nanotube-like structure are possible. Additionally, there is potential to exploit the cis conformation in interesting supramolecular chemistry applications. Furthermore, we report that a directly linked CPP dimer can adopt a stable cis conformation. We are currently investigating the synthesis of directly linked CPP dimers, as well as cyclodehydrogenation reactions of arene-linked dimers **1** and **2**. We will report the results of these investigations in due course.

EXPERIMENTAL SECTION

Bromo-Substituted Macrocycle 7. Diiodide **5** (1.25 g, 2.00 mmol), diboronate **6** (1.52 g, 2.00 mmol), Pd(OAc)₂ (135 mg, 0.200 mmol, 0.1 equiv) and Cs₂CO₃ (2.61 g, 8.00 mmol, 4 equiv) were charged in a 500 mL Schlenk flask under nitrogen, then degassed DMF (350 mL) and 2-isopropanol (35 mL) was added. The resulting mixture was heated to 100 °C and stirred for 24 h. After cooling down to room temperature, the mixture was filtered through a short plug of Celite, and 250 mL water was added to the filtrate. After extraction with dichloromethane (3 × 100 mL), the combined organic phase was washed with water (8 × 100 mL) and dried over sodium sulfate. After removing the solvent under vacuum, the crude mixture was purified by silica column chromatography (ethyl acetate/hexane = 2:3) to give the brominated [8]macrocycle **7** as a white solid (530 mg, 30%, mp 155 °C.). ¹H NMR (400 MHz, CDCl₃): δ(ppm) 7.45–7.53 (m, 14H, Ar), 7.35 (d, *J* = 8.4 Hz, 2H, Ar), 7.23 (t, *J* = 8.8 Hz, 2H, Ar), 7.08 (d, *J* = 8 Hz, 2H, Ar), 6.79 (d, *J* = 1.6 Hz, 1H, Vinyl-H), 6.23–6.26 (m, 2H, Vinyl-H), 6.12–6.15 (overlap, 4H, Vinyl-H), 6.04–6.08 (overlap, 4H, Vinyl-H), 3.47–3.49 (overlap, 12H, OMe), 3.40 (s, 6H, OMe). ¹³C NMR (100 MHz, CDCl₃): δ(ppm) 143.35, 143.31, 143.02, 142.85, 140.53, 140.11, 139.46, 139.43, 139.40, 138.70, 138.30, 134.55,

133.72, 133.48, 133.46, 133.30, 132.98, 132.80, 132.76, 132.61, 131.32, 128.10, 127.30, 127.18, 127.15, 126.87, 126.79, 126.38, 126.31, 126.24, 104.96, 78.83, 78.78, 74.59, 74.51, 74.02, 73.96, 52.43 (OMe), 52.12, 52.09, 51.80. MALDI-TOF *m/z* calcd for C₅₄H₄₀BrO₆ (M)⁺: 873.87, found (isotopic pattern): 872.1226, 874.1280, 875.1285. IR (neat): 736, 772, 820, 949, 1005, 1016, 1080, 1174, 1265, 1397, 1449, 1491, 2823, 2932 cm⁻¹.

Phenyl-bridged Macrocycle 10. A mixture of brominated [8]macrocycle **7** (288 mg, 0.330 mmol), 1,4-benzenediboric acid bis(pinacol) ester **8** (50.0 mg, 0.150 mmol), Pd(PPh₃)₄ (38.0 mg, 0.0330 mmol) and Cs₂CO₃ (430 mg, 1.32 mmol) was dissolved in Toluene/H₂O (7 mL, 6:1) and stirred at 80 °C for 24 h under nitrogen. After cooling down to room temperature, 10 mL water was added. The aqueous phase was extracted with dichloromethane (3 × 10 mL) and the combined organics were washed with water (3 × 10 mL) and dried over sodium sulfate. After removing the solvent under vacuum, the crude mixture was purified by silica column chromatography (ethyl acetate/hexane = 1:1) to give **10** as a white solid (165 mg, 66%, d.p. > 300 °C.). ¹H NMR (400 MHz, CDCl₃): δ(ppm) 7.47–7.52 (m, 20H, Ar), 7.40 (d, *J* = 8.4 Hz, 4H, Ar), 7.27 (d, *J* = 6 Hz, 8H, Ar), 7.20 (d, *J* = 6 Hz, 8H, Ar), 7.04 (d, *J* = 8.8 Hz, 4H, Ar), 6.68 (d, *J* = 2 Hz, 2H, Vinyl-H), 6.02–6.21 (overlap, 20H, Vinyl-H), 3.40–3.48 (overlap, 30H, OMe), 3.12 (s, 6H, OMe). ¹³C NMR (100 MHz, CDCl₃): δ(ppm) 143.30, 142.80, 142.72, 140.86, 140.25, 140.21, 139.67, 139.49, 139.45, 139.34, 138.18, 136.69, 135.57, 134.00, 133.51, 133.40, 133.19, 133.10, 132.81, 132.32, 128.82, 127.58, 127.22, 126.97, 126.83, 126.73, 126.59, 126.49, 126.23, 126.18, 78.78, 76.30, 74.58, 74.54, 74.05, 74.03, 52.10 (OMe), 51.97, 51.84, 51.69. MALDI-TOF *m/z* calcd for C₁₁₄H₁₀₂O₁₂ (M)⁺: 1664.02. Found: 1664.3682. IR (neat): 819, 950, 1016, 1079, 1174, 1491, 2822, 2931 cm⁻¹.

Naphthyl-bridged Dimer 11. A mixture of brominated [8]macrocycle **7** (73.2 mg, 0.0840 mmol), 1,5-naphthalenediboric acid bis(pinacol) ester **9** (16.0 mg, 0.0420 mmol), Pd(PPh₃)₄ (9.70 mg, 0.00840 mmol) and Cs₂CO₃ (110 mg, 0.340 mmol) was dissolved in Toluene/H₂O (2 mL, 6:1) and

stirred at 90 °C for 24 h under nitrogen. After cooling down to room temperature, 5 mL water was added. The aqueous phase was extracted with dichloromethane (3 × 5 mL) and the combined organics were washed with water (3 × 5 mL) and brine (5 mL) and dried over sodium sulfate. After removing the solvent under vacuum, the crude mixture was purified by silica column chromatography (ethyl acetate/hexane = 30% to 50%) to give compound **11** as an off-white solid (35 mg, 49%, d.p. > 300 °C). ¹H NMR (400 MHz, CDCl₃): δ(ppm) 8.28 (br s, 1H, Ar), 7.53–7.47 (overlap, 28H, Ar), 7.29–7.27 (overlap, 8H, Ar), 7.12–7.00 (overlap, 9H, Ar), 6.61 (br d, 2H, vinyl-H), 6.46 (d, *J* = 10.5 Hz, 2H, vinyl-H), 6.36 (d, *J* = 10.5 Hz, 2H, vinyl-H), 6.17–6.05 (overlap, 16H, vinyl-H), 3.59 (overlap, 6H, OMe), 3.49 (overlap, 12H, OMe), 3.48 (overlap, 12H, OMe), 3.26 (overlap, 6H, OMe); ¹³C NMR (125 MHz, CDCl₃): δ(ppm) 143.32, 142.96, 142.87, 140.77, 140.40, 140.36, 139.78, 139.52, 139.41, 137.04, 136.14, 135.47, 133.94, 133.55, 133.50, 133.25, 133.12, 133.05, 132.87, 132.75, 132.37, 128.05, 127.62, 127.44, 126.94, 126.76, 126.36, 126.32, 126.28, 126.24, 126.22, 125.42, 124.26, 79.81, 76.41, 74.63, 74.52, 74.13, 74.10, 52.76, 52.51, 52.11, 51.86. MALDI-TOF *m/z* calcd for C₁₁₈H₁₀₄O₁₂ (M)⁺: 1714.08, Found: 1713.4715. IR(neat): 729, 819, 950, 1016, 1079, 1174, 1490, 2822, 2934 cm⁻¹.

Preparation of Sodium Naphthalenide (1.0 M in THF). To a 25 mL dry round-bottom flask charged with a solution of naphthalene (768 mg, 6.00 mmol) in 6 mL dry THF was added sodium metal (207 mg, 9.00 mmol) under nitrogen. The reaction mixture was stirred for 18 h at room temperature. After this time, a green solution containing sodium naphthalenide (1.0 M in THF) was formed.

Phenyl-bridged CPP Dimer 1. Compound **10** (150 mg, 0.0900 mmol) was dissolved in 15 mL THF under nitrogen and cooled down to -78 °C. At this point, the freshly prepared sodium naphthalenide (1.62 mL, 1.62 mmol, 1.0 M in THF) was added. The reaction mixture was stirred for 2 h at -78 °C before the addition of I₂ (1.5 mL of a 1 M solution in THF). Then the resulting mixture was warmed up to room temperature and sodium thiosulfate (saturated solution) was carefully added to remove excess I₂. Water (30 mL) was then added and the mixture was extracted with dichloromethane (3 ×). After removing the solvent under reduced pressure, the crude yellow solid was purified by chromatography (chlorobenzene/hexanes = 4:1) to give compound **1** as a yellow solid (88 mg, 75%, d.p. > 350 °C). ¹H NMR (400 MHz, CDCl₃): δ(ppm) 7.93 (m, 2H), 7.75 (s, 4H), 7.55 (overlap, 14H), 7.47 (overlap, 34H), 7.38 (overlap, 4H), 7.09 (overlap, 8H). ¹³C NMR (100 MHz, CDCl₃+CS₂): δ(ppm) 140.19, 137.33 (multiple overlapping peaks), 127.11 (multiple overlapping peaks). MALDI-TOF *m/z* calcd for C₁₀₂H₆₆ (M)⁺: 1291.62. Found: 1291.5924. IR (neat): 735, 815, 1261, 1482, 1587, 2335, 2360, 2851, 2924, 3018 cm⁻¹.

Naphthyl-Bridged CPP Dimer 2. Compound **11** (35.0 mg, 0.0200 mmol) was dissolved in 3 mL THF under nitrogen and cooled down to -78 °C. At this point, the freshly prepared sodium naphthalenide (0.360 mL, 0.360 mmol, 1.0 M in THF) was added. The reaction mixture was stirred for 2 h at -78 °C before the addition of I₂ (1 mL of a 1 M solution in THF). Then the resulting mixture was warmed up to room temperature and sodium thiosulfate (saturated solution) was carefully added to remove excess I₂. Water (30 mL) was then added and the mixture was extracted with dichloromethane (3 × 20 mL), which was combined and washed brine (30 mL) and dried over sodium sulfate. At this point, the freshly prepared

ssure, the crude yellow solid was purified by chromatography (hexanes/dichloromethane = 2:3) to give compound **2** as a yellow solid (13 mg, 48%, d.p. > 350 °C). ¹H NMR (400 MHz, CDCl₃): δ(ppm) 8.00 (m, 1H), 7.82 (overlap, 2H), 7.68 (br s, 1H) 7.49 (overlap, 54H), 7.14 (overlap, 8H), 7.01 (overlap, 2H). ¹³C NMR (100 MHz, CDCl₃): δ(ppm) 137.38–138.23 (multiple overlapping peaks), 127.38 (multiple overlapping peaks). MALDI-TOF *m/z* calcd for C₁₀₆H₆₈ (M)⁺: 1341.67, Found: 1341.1713. IR(neat): 729, 815, 1074, 1262, 1482, 1586, 2364, 2980, 3021.

■ ASSOCIATED CONTENT

● Supporting Information

General experimental considerations, syntheses and characterization of all new compounds, UV–vis, fluorescence, and cyclic voltammetry spectra, details of calculations, and movie of conformational change. This material is available free of charge via the Internet at <http://pubs.acs.org>.

■ AUTHOR INFORMATION

Corresponding Author

*E-mail: jasti@bu.edu.

Notes

The authors declare no competing financial interest.

■ REFERENCES

- (1) Iijima, S. *Nature* **1991**, *354*, 56.
- (2) Dresselhaus, M. S. D., G.; Avouris, P. *Carbon Nanotubes: Synthesis, Structure, Properties and Applications*; Springer-Verlag: Berlin, 2001.
- (3) Jose-Yacamán, M.; Miki-Yoshida, M.; Rendon, L.; Santiesteban, J. G. *Appl. Phys. Lett.* **1993**, *62*, 657.
- (4) Thess, A.; Lee, R.; Nikolaev, P.; Dai, H.; Petit, P.; Robert, J.; Xu, C.; Lee, Y. H.; Kim, S. G.; Rinzler, A. G.; Colbert, D. T.; Scuseria, G. E.; Tománek, D.; Fischer, J. E.; Smalley, R. E. *Science* **1996**, *273*, 483.
- (5) Prasek, J.; Drbohlavova, J.; Chomoucka, J.; Hubalek, J.; Jasek, O.; Adam, V.; Kizek, R. *J. Mater. Chem.* **2011**, *21*, 15872.
- (6) Bodwell, G. *Nat. Nanotechnol.* **2010**, *5*, 103.
- (7) Jasti, R.; Bertozzi, C. R. *Chem. Phys. Lett.* **2010**, *494*, 1.
- (8) Tian, X.; Jasti, R. In *Fragments of Fullerenes and Carbon Nanotubes: Designed Synthesis, Unusual Reactions, and Coordination Chemistry*; Petrukhina, M. A., Scott, L. T., Eds.; Wiley: 2011.
- (9) Scott, L. T. *Polycyclic Aromat. Compd.* **2010**, *30*, 247.
- (10) Fort, E. H.; Donovan, P. M.; Scott, L. T. *J. Am. Chem. Soc.* **2009**, *131*, 16006.
- (11) Steinberg, B.; Scott, L. *Angew. Chem., Int. Ed.* **2009**, *48*, 5400.
- (12) Fort, E. H.; Scott, L. T. *Angew. Chem., Int. Ed.* **2010**, *49*, 6626.
- (13) Fort, E. H.; Scott, L. T. *J. Mater. Chem.* **2011**, *21*, 1373.
- (14) Li, H.-B.; Page, A.; Irle, S.; Morokuma, K. *ChemPhysChem* **2012**, *13*, 1479.
- (15) Kim, J.; Page, A.; Irle, S.; Morokuma, K. *J. Am. Chem. Soc.* **2012**, *134*, 9311.
- (16) Omachi, H.; Segawa, Y.; Itami, K. *Acc. Chem. Res.* **2012**, *45*, 1378.
- (17) Bunz, U.; Menning, S.; Martín, N. *Angew. Chem., Int. Ed.* **2012**, *51*, 7094.
- (18) Schrettl, S.; Frauenrath, H. *Angew. Chem., Int. Ed.* **2012**, *51*, 6569.
- (19) Page, A.; Ohta, Y.; Irle, S.; Morokuma, K. *Acc. Chem. Res.* **2010**, *43*, 1375.
- (20) Segawa, Y.; Fukazawa, A.; Matsuura, S.; Omachi, H.; Yamaguchi, S.; Irle, S.; Itami, K. *Org. Biomol. Chem.* **2012**, *10*, 5979.
- (21) Iwamoto, T.; Watanabe, Y.; Sakamoto, Y.; Suzuki, T.; Yamago, S. *J. Am. Chem. Soc.* **2011**, *133*, 8354.
- (22) Jasti, R.; Chattarjee, J.; Neaton, J. B.; Bertozzi, C. R. *J. Am. Chem. Soc.* **2008**, *130*, 17646.

- (23) Sisto, T. J.; Golder, M. R.; Hirst, E. S.; Jasti, R. *J. Am. Chem. Soc.* **2011**, *133*, 15800.
- (24) Xia, J.; Jasti, R. *Angew. Chem., Int. Ed.* **2012**, *51*, 2474.
- (25) Xia, J.; Bacon, J. W.; Jasti, R. *Chem. Sci.* **2012**, *3*, 3018.
- (26) Wong, B. M. *J. Phys. Chem. C* **2009**, *113*, 21921.
- (27) Iwamoto, T.; Watanabe, Y.; Sadahiro, T.; Haino, T.; Yamago, S. *Angew. Chem., Int. Ed.* **2011**, *50*, 8342.
- (28) Parekh, V. C.; Guha, P. C. *J. Indian. Chem. Soc.* **1934**, *11*, 95.
- (29) Friederich, R.; Nieger, M.; Vögtle, F. *Chem. Ber* **1993**, *126*, 1723.
- (30) Darzi, E. R.; Sisto, T. J.; Jasti, R. *J. Org. Chem.* **2012**, *77*, 6624.
- (31) Takaba, H.; Omachi, H.; Yamamoto, Y.; Bouffard, J.; Itami, K. *Angew. Chem., Int. Ed.* **2009**, *48*, 6112.
- (32) Omachi, H.; Matsuura, S.; Segawa, Y.; Itami, K. *Angew. Chem., Int. Ed.* **2010**, *49*, 10202.
- (33) Segawa, Y.; Miyamoto, S.; Omachi, H.; Matsuura, S.; Šenel, P.; Sasamori, T.; Tokitoh, N.; Itami, K. *Angew. Chem., Int. Ed.* **2011**, *50*, 3244.
- (34) Segawa, Y.; Šenel, P.; Matsuura, S.; Omachi, H.; Itami, K. *Chem. Lett.* **2011**, *40*, 423.
- (35) Yuuki, I.; Yusuke, N.; Haruka, O.; Sanae, M.; Katsuma, M.; Hisanori, S.; Yasutomo, S.; Kenichiro, I. *Chem. Sci.* **2012**, *3*, 2340.
- (36) Yamago, S.; Watanabe, Y.; Iwamoto, T. *Angew. Chem., Int. Ed.* **2010**, *49*, 644.
- (37) Kayahara, E.; Sakamoto, Y.; Suzuki, T.; Yamago, S. *Org. Lett.* **2012**, *14*, 3284.
- (38) For some related structures see: (a) Hitosugi, S.; Nakanishi, W.; Yamasaki, T.; Isobe, T. *Nat. Commun.* **2011**, *2*, 1505. (b) Omachi, H.; Segawa, Y.; Itami, K. *Org. Lett.* **2011**, *13*, 2480. (c) Yagi, A.; Segawa, Y.; Itami, K. *J. Am. Chem. Soc.* **2012**, *134*, 2962. (d) Hitosugi, S.; Yamasaki, T.; Isobe, H. *J. Am. Chem. Soc.* **2012**, *134*, 12442. (e) Matsui, K.; Segawa, Y.; Itami, K. *Org. Lett.* **2012**, *14*, 1888. (f) Matsui, K.; Segawa, Y.; Namikawa, T.; Kamada, K.; Itami, K. *Chem. Sci.* **2012**, DOI: 10.1039/C2SC21322B. (g) Sisto, T. J.; Tian, X.; Jasti, R. *J. Org. Chem.* **2012**, *77*, 5857. (h) Scott, L. T.; Jackson, E. A.; Zhang, Q.; Steinberg, B. D.; Bancu, M.; Li, B. *J. Am. Chem. Soc.* **2012**, *134*, 107.
- (39) Chuang, K. V.; Navarro, R.; Reisman, S. E. *Chem. Sci.* **2011**, *2*, 1086.
- (40) Mo, F.; Jiang, Y.; Qiu, D.; Zhang, Y.; Wang, J. *Angew. Chem., Int. Ed.* **2010**, *49*, 1846.
- (41) Gómez-López, M.; Preece, J. A.; Stoddart, J. F. *Nanotechnology* **1996**, *7*, 183.
- (42) Balzani, V.; Credi, A.; Raymo, F. M.; Stoddart, J. F. *Angew. Chem., Int. Ed.* **2000**, *39*, 3348.
- (43) Pease, A. R.; Jeppesen, J. O.; Stoddart, J. F.; Luo, Y.; Collier, C. P.; Heath, J. R. *Acc. Chem. Res.* **2001**, *34*, 433.
- (44) Tseng, H.-R.; Vignon, S. A.; Stoddart, J. F. *Angew. Chem., Int. Ed.* **2003**, *42*, 1491.
- (45) Badjić, J. D.; Balzani, V.; Credi, A.; Silvi, S.; Stoddart, J. F. *Science* **2004**, *303*, 1845.
- (46) Moonen, N.; Flood, A.; Fernández, J.; Stoddart, J. *Top. Curr. Chem.* **2005**, *262*, 99.
- (47) Landge, S. M.; Aprahamian, I. *J. Am. Chem. Soc.* **2009**, *131*, 18269.
- (48) Because this data could not be refined to publishable quality, interested readers should contact the authors directly.
- (49) Wong, B. M. *Comput. Chem.* **2009**, *30*, 51.
- (50) Osuna, S.; Swart, M.; Solà, M. *J. Phys. Chem. A* **2011**, *115*, 3491.
- (51) For a full analysis of all optical transitions for dimers 1 and 2, see Tables S2–S5 in the Supporting Information.